

## Numerical Analysis of Torsionally Loaded Drilled Shafts Near an Embankment Slope in Cohesionless Soils

Alina Irsainova, Aigul Mussabayeva, Sudheesh Thiyya Kkand and Jong Kim  
Department of Civil Engineering, Nazarbayev University, Kabanbay Batyr Avenue 53,  
010000 Astana, Kazakhstan

**Abstract:** Foundations for mast arm/overhead cantilever structures supporting highway signs, signals and luminaires in hurricane prone areas should be sufficient to resist the torsion and lateral load caused by severe wind loading. In some instances such structures are to be installed on top of highway Embankment and the proximity of Embankment slope may adversely influence the torque resistance of the foundation. However, the degree of reduction in torsional resistance due to the closeness of a slope was unknown. A numerical investigation of drilled shaft foundations supporting mast arm structures located near an Embankment slope in cohesionless soils was performed. The torque resistance was found to reduce by a maximum of 22% when the slope angle was varied from  $0^\circ$ - $34^\circ$  (i.e., 0-1 V:1.5H). The study revealed that the degree of reduction is a function of the Embankment height and the distance between the shaft face and the crest line whereas, independent of the friction angle of soil. It was also identified that the equivalent level ground approach typically used in the industry practice is adequate for smaller Embankment heights but over-predicts in case of larger Embankments.

**Key words:** Drilled shafts, torsion, slope, cohesionless soils, proximity of Embankment

### INTRODUCTION

Drilled shaft foundations are generally used to support the miscellaneous structures such as mast arms and overhead structures for supporting highway signs, signals and luminaires (NCHRP, 2003). The drilled shafts supporting such cantilever type structures are subjected to high torsion and lateral loads under heavy wind velocity (e.g., hurricane). Past studies have shown that such structures should be designed for a coupled torque-lateral load scenario (Herrera, 2001; Hu *et al.*, 2006; McVay *et al.*, 2003; Tawfiq, 2000; Thiyyakkandi, *et al.*, 2016). Specifically, the lateral resistance of the foundation is found to be significantly reduced by the impact of coexisting torsion whereas, the torsional resistance remains nearly the same irrespective of the magnitude of lateral load.

Sometimes the mast arms/overhead sign structures are required to be installed near/on the slope of highway Embankments. It is obvious that the proximity of a slope will influence the torsional and lateral capacity of the foundations. There are several studies reported on the lateral resistance of pile near the slope (Lee *et al.*, 2006) resistance of pile. The typical industry practice in the southeastern united states is to consider only the portion

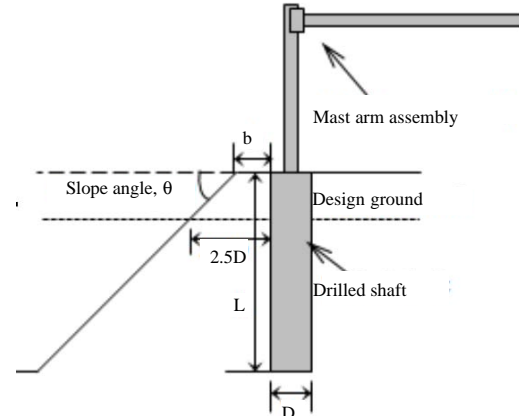


Fig. 1: Schematic of a mast arm foundation near an Embankment slope

of pile/shaft with a minimum horizontal soil cover (from pile face to slope face) of  $2.5D$  for the estimation of the torsional resistance as if founded in level ground (Fig. 1). However, whether this approach is reasonable or not is presently unknown.

This research investigated the reduction in torque resistance of shaft/pile in cohesionless soils due to the immediacy of an Embankment slope through numerical

modeling. The influence of slope angle, Embankment height, distance from crest line to shaft face and angle of internal friction of soil on the degree of reduction of torque resistance was identified. Adequacy of the equivalent level ground approach for estimating the torque resistance of piles/shafts adjacent to slopes was also checked.

## MATERIALS AND METHODS

**Numerical modeling:** The three-dimensional (3D) finite-element program, PLAXIS 3D, developed by PLAXIS b.v., Netherlands was used for the numerical modeling. In order to simulate the actual structural and loading conditions, the drilled shafts supporting full-scale mast arm assembly (pole and mast arm) were modeled. The drilled shaft, mast arm assembly and sand were simulated with 10-noded solid elements (Fig. 2). The drilled shaft and pole-mast arm assembly were modeled as linear elastic materials and the sand was modeled with mohr-coulomb material model.

**Validation of model:** First of all, the PLAXIS 3D package was validated by simulating the centrifuge tests on the drilled shaft supporting mast arm structure in dry sand with flat ground (i.e., no slope) reported by McVay *et al.* (2003). Table 1 presents the relevant details of their study and so used for the validation. The torsion on foundation was simulated by applying a lateral load on the mast arm at an eccentric distance of 4.4 m from the pole (Fig. 2) as done in the centrifuge tests (McVay *et al.*, 2003). It should be noted that the application of lateral load at an eccentric distance will develop torsion on the foundation in the present case torsion = applied lateral load x 4.4 m (Fig. 3) compares the torque-rotation responses obtained from the numerical analysis and the centrifuge tests. It is evident from the figure that the results from the finite element analysis were in good agreement with the centrifuge results.

**Numerical analysis with the variation of parameters:** Following the validation of the PLAXIS Model, several numerical analyses were performed by varying the angle of slope, length, diameter and L/D ratio of shaft, friction angle of soil and the distance from crest line to drilled shaft (b). Table 2 lists the parametric variations considered in the study. The unit weight (17 kN/m<sup>3</sup>) and Poisson's ratio (0.25) of sand were kept constant for all the analyses.

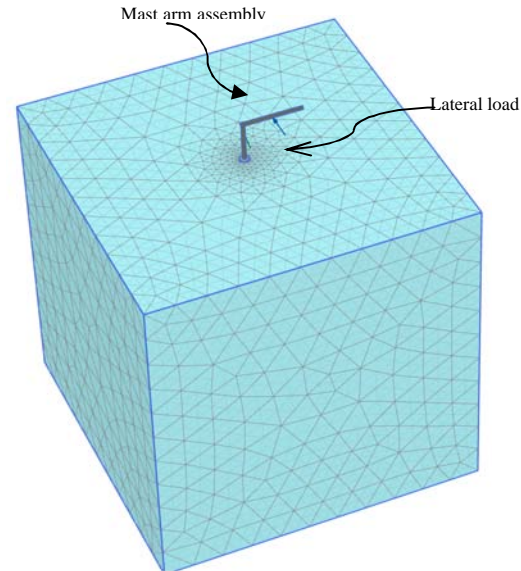


Fig. 2: FE simulation of centrifuge tests conducted by McVay *et al.* (2003)

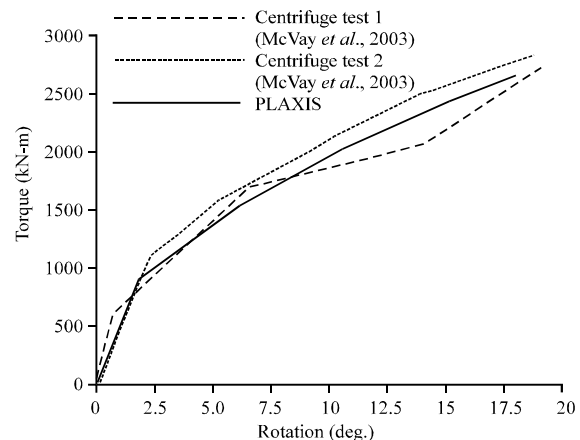


Fig. 3: Validation of PLAXIS Model

Table 1: Relevant details of the centrifuge tests used for the validation of PLAXIS Model

| Particulars   | Parameters                                      | Values            |
|---------------|---|-------------------|
| Drilled shaft | Diameter (D) (m)                                | 1.52              |
|               | Length (L) (m)                                  | 10.7              |
|               | Unit weight ( $\gamma_s$ ) (kN/m <sup>3</sup> ) | 25                |
|               | Modulus of elasticity ( $E_c$ ) (kPa)           | $1.7 \times 10^7$ |
| Mast arm      | Pole height (m)                                 | 6.1               |
|               | Arm length (m)                                  | 9.1               |
|               | Unit weight ( $\gamma_m$ ) (kN/m <sup>3</sup> ) | 75                |
|               | Modulus of elasticity ( $E_m$ ) (kPa)           | $2.0 \times 10^8$ |
| Sand          | Angle of internal angle ( $\phi$ ) (deg.)       | 34.7              |
|               | Unit weight ( $\gamma_s$ ) (kN/m <sup>3</sup> ) | 15                |
|               | Interface friction angle ( $\delta$ ) (deg.)    | $2/3\phi = 23.2$  |
|               | Cohesion (c) (kPa)                              | 0                 |
|               | Modulus of elasticity ( $E_s$ ) (kPa)           | $6.0 \times 10^4$ |
|               | Poisson's ratio ( $\nu$ )                       | 0.25              |

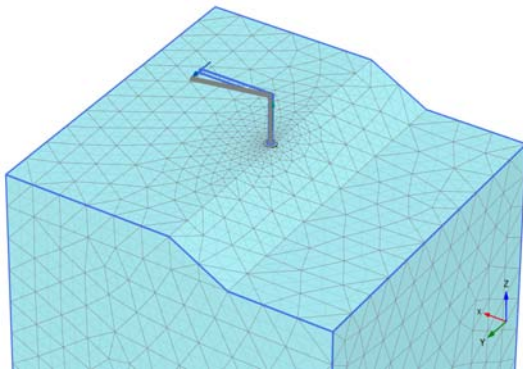


Fig. 4: Typical PLAXIS 3D Model for structure near a slope (V:H = 1:2, D = 1 m, L/D = 7, b = 0)

Table 2: Range of parameters considered in the study

| Parameters               | Values                                     |
|--------------------------|--|
| $\theta$ (deg.) or (V:H) | 0, 18.4 (1:3), 26.6 (1:2) and 33.7 (1:1.5) |
| D (m)                    | 1 and 1.5                                  |
| L (m)                    | 3, 4.5, 5, 7, 7.5 and 10.5                 |
| L/D                      | 3, 5 and 7                                 |
| $\phi$ (deg.)            | 30, 32 and 34                              |
| b (m)                    | 0, 1D and 2D                               |

The initial soil stress state due to gravity loading was considered in the analyses. However, the variation stress state due to the shaft construction (i.e., installation effect) was not accounted in the present study. Interface elements were used to model the soil-shaft interaction during the loading. The properties of shaft-sand interface were set to the surrounding sand with a strength reduction/rigidity factor of 0.67. For all the analyses, the bottom of Embankment was considered at the tip elevation of the drilled shaft; i.e., height of Embankment is equal to the length of shaft (L). The water table was assumed to be below the toe of Embankment. Default boundary conditions in PLAXIS 3D (free field condition) were used for all the cases.

A mast arm assembly with 6 m high pole and 10 m long arm (same properties as in Table 1) was considered for the parametric study. The lateral load was applied at the end of arm (i.e., eccentricity = 10 m) to minimize the required lateral load to cause the torsional failure (Fig. 4). The torsional resistance corresponding to  $10^\circ$  of rotation was used consistently for further analysis and comparison.

## RESULTS AND DISCUSSION

Figure 5 presents the variation of torque resistance with the angle of slope for different L/D ratios and friction angles in case of a 1m-diameter drilled shaft located at the crest line (i.e., b = 0). As expected, the torsional resistance

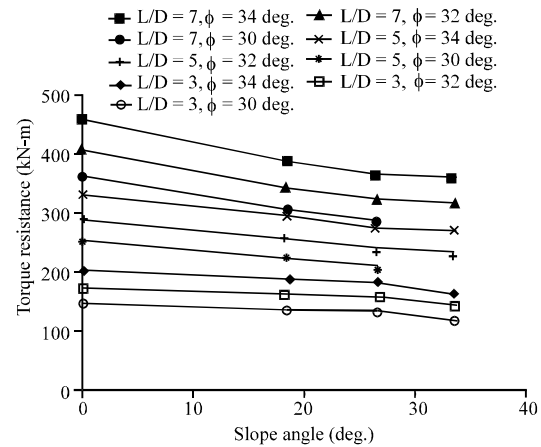


Fig. 5: Variation of torque resistance with slope angle (D = 1 m and b = 0)

has decreased with the increase of slope angle for all the cases. It is also evident from Fig. 5 that the rate of variation was independent of the angle of internal friction of soil. However, the L/D ratio which reflects the height of Embankment (equal to shaft length) was found to slightly influence the reduction in torsional resistance.

For more convenience, the estimated torsional resistance values were normalized by dividing with the maximum torsional resistance (i.e. for  $\theta = 0$ ) for each case. The ratio of the torque resistance for a given  $\theta$  to the maximum torque resistance ( $\theta = 0$ ) is referred to here as torque ratio ( $R_{\text{torque}}$ ). The torque ratio vs. slope angle for different L/D ratios and shaft diameters (D) for the case of b = 0 are shown in Fig. 6. It can be seen from the Figure that the variation of torque ratios for all the cases falls in a narrow range. Specifically, a maximum reduction of 22% ( $R_{\text{torque}} = 0.78$ ) was observed as the slope angle varied from 0-34°.

Figure 7 displays the reduction in torque ratio with the angle of slope for b = 0, 1D and 2D. The reduction in torque resistance was found to be a function of the location of the drilled shaft with respect to the crest line of the Embankment as expected. However, the difference in the reduction was not significant; minimum  $R_{\text{torque}}$  were 0.78, 0.83 and 0.87, respectively for b = 0, 1D and 2D.

It was also of interest to compare the estimated torque resistance for different slope angles with that based on equivalent level ground approach typically used in industry (Fig. 1). Firstly, the equivalent design ground corresponding to each slope angle was estimated as shown in Fig. 1 by considering a minimum horizontal soil cover of 2.5D. Subsequently, the numerical analysis was performed with the equivalent flat ground model. Note that the embedment depth of the shaft was smaller than

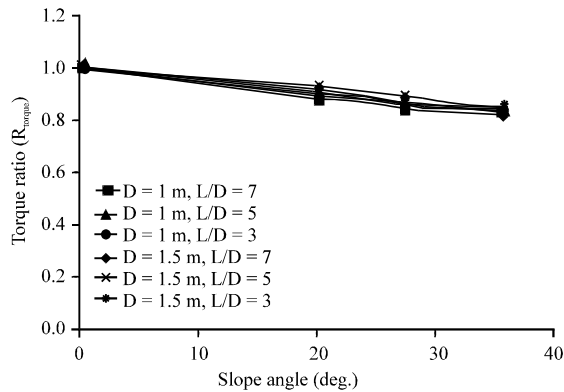


Fig. 6: Reduction in torque ratio with slope angle ( $b = 0$ )

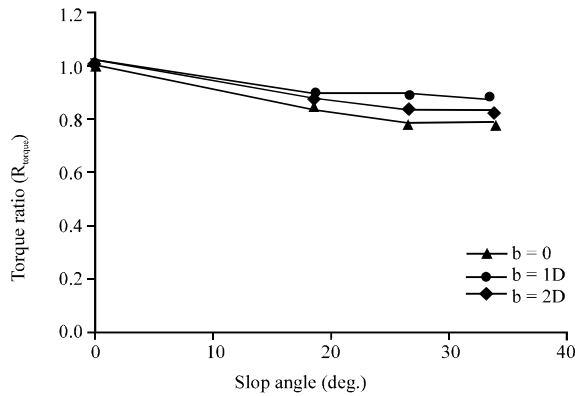


Fig. 7: Reduction in torque ratio with slope angle ( $D = 1 \text{ m}$ ,  $L/D = 7$ )

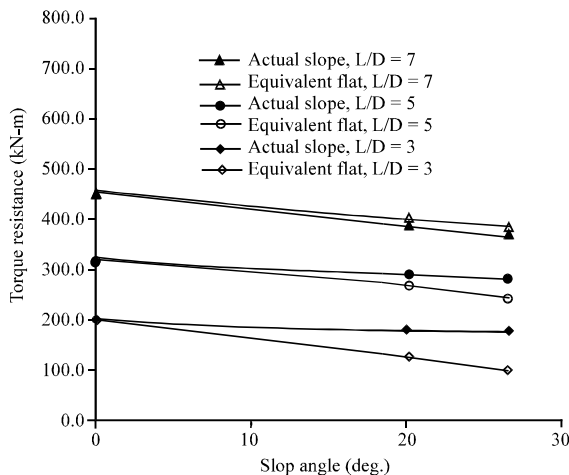


Fig. 8: Comparison of equivalent level ground results with the actual slope results ( $D = 1 \text{ m}$ ,  $L/D = 7$ ,  $b = 0$ )

the shaft length ( $L$ ) as the portion of the shaft with the soil cover  $< 2.5D$  in the actual scenario will be above the design ground in the equivalent level ground approach.

Figure 8 compares the torsional resistance of shafts in the actual sloped case and the equivalent flat ground case. The difference was found to increase with the increase of the slope angle. It is evident from the figure that the equivalent flat ground approach under-predicts the available resistance for smaller Embankment heights (e.g.,  $L/D = 3$  and  $5$ ) and over-predicts for larger Embankments (e.g.,  $L/D \geq 7$ ). This suggests that the simplified approach is reasonable for smaller Embankment cases whereas, special care should be taken when used for foundations on taller Embankments.

## CONCLUSION

This study presents a numerical study carried out to quantify the influence of an Embankment slope on the torsional resistance of drilled shafts. The finite element software, PLAXIS 3D was used to model the mast arm structures supported by drilled shafts foundation in cohesionless soils. The study showed a maximum reduction in torsional resistance of 22% with the variation of the slope angle from  $0^\circ$ - $34^\circ$ . The Embankment slope angle, height and the distance from the shaft face to the crest line are found to control the percentage of reduction. However, the reduction was not influenced by the angle of internal friction of the Embankment materials.

Numerical analyses for different slope angles with respective equivalent flat ground suggested that the simplified design ground approach is adequate for smaller Embankments ( $L/D < 7$ ); however not acceptable for large Embankment heights. Since these findings are solely based on the numerical modeling, further validation is warranted by laboratory (e.g., centrifuge) or field load testing.

## NOMENCLATURE

- $D$  = Diameter of drilled shaft (m)
- $\phi$  = Angle of internal friction of sand (deg.)
- $L$  = Length of drilled shaft = Height of Embankment (m)
- $\delta$  = Fiction angle at shaft-sand interface (deg.)
- $b$  = Distance from crest line to drilled shaft (m)
- $\nu$  = Poisson's ratio of sand
- $\theta$  = Slope angle
- $\gamma_s$  = Unit weight of sand ( $\text{kN/m}^3$ )
- $E_s$  = Modulus of elasticity of sand (kPa)
- $\gamma_c$  = Unit weight of concrete ( $\text{kN/m}^3$ )
- $E_c$  = Modulus of elasticity of concrete (kPa)
- $\gamma_m$  = Unit weight of mast arm steel ( $\text{kN/m}^3$ )
- $E_m$  = Modulus of elasticity of mast arm steel (kPa)

## REFERENCES

- Herrera, R., 2001. Determine optimum depths of drilled shafts subjected to combined torsion and lateral loads using the centrifuge. Master Thesis, University of Florida, Gainesville, Florida.
- Hu, Z., M. McVay, D. Bloomquist, R. Herrera and P. Lai, 2006. Influence of torque on lateral capacity of drilled shafts in sands. *J. Geotech. Geoenviron. Eng.*, 132: 454-464.
- Lee, S.W., A.R. Pickles and T.O. Henderson, 2006. Numerical modeling of laterally loaded short pile. *Proceedings of the 6th European Conference on Numerical Methods in Geotechnical Engineering*, September 6-8, 2006, Taylor & Francis, Graz, Austria, ISBN:978-0-415-40822-6, pp: 557-561.
- McVay, M., R. Herrera and Z. Hu, 2003. Determine optimum depths of drilled shafts subject to combined torsion and lateral loads using centrifuge testing (BC-354, RPWO #9). Master Thesis, Florida State University, Tallahassee, Florida.
- NCHRP, 2003. Structural supports for highway signs, luminaires and traffic signals (NCHRP report 494). National Cooperative Highway Research Program, TRB, Washington, USA.
- Tawfiq, K., 2000. Drilled shafts under torsional loading conditions (B-9191). Master Thesis, Florida Department of Transportation, Florida State University, Tallahassee, Florida.
- Thiyyakkandi, S., M. McVay, P. Lai and R. Herrera, 2016. Full-scale coupled torsion and lateral response of mast arm drilled shaft foundations. *Can. Geotech. J.*, 53: 1928-1938.